QCD STRUCTURE OF THE ELECTRON* **

W. Słomiński and J. Szwed

Institute of Computer Science, Jagellonian University
Reymonta 4, 30-059 Kraków, Poland

(Received April 6, 1998)

The concept of the QCD structure of electron is presented. Advantages of the electron structure function over that of the photon are demonstrated in the electron induced processes. At very high momenta probabilistic interpretation can be preserved despite strong γ-Z interference.

PACS numbers: 13.60. –r, 14.60. –z

The QCD structure of the photon is revealed in interactions with a highly virtual 'probe', *e.g.* a virtual photon or a virtual gluon. The distribution of quarks and gluons seen by this probe inside the photon is described by the photon structure function. The theoretical and phenomenological predictions for this function are known since long [1]. At present the data on the photon structure are measured in experiments where the electron serves as a target [2]. To fix our attention let us think of electron-positron scattering, where a highly virtual photon from the positron hits the photon emitted by the electron. The process is depicted in Fig. 1a. The black blob denotes 'resolved' photon and sums up all QCD contributions. The photon emitted by the electron is, in fact, also virtual and, from the point of view of a physical process, γ^* measures the structure (parton content) of the electron, as depicted in Fig. 1b.

In the following we will demonstrate the advantages of introducing the electron structure function. We will consider it as a more adequate means to describe the actual experimental situation and, at very high energies, as the method to preserve partonic interpretation of the cross-section.

---

* Presented at the Cracow Epiphany Conference on Spin Effects in Particle Physics and Tempus Workshop, Cracow, Poland, January 9–11, 1998.

** Work supported by the Polish State Committee for Scientific Research (grant No. 2 P03B 081 09) and the Volkswagen Foundation.

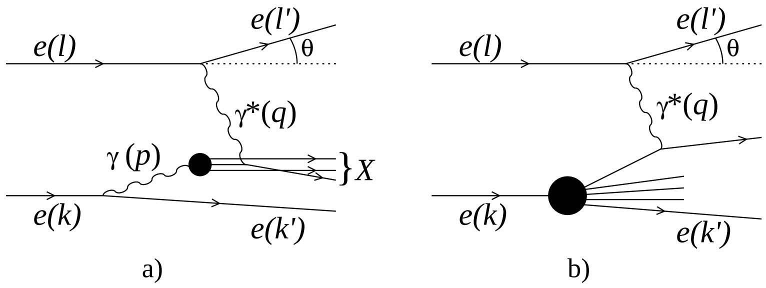

Fig. 1. Deep inelastic scattering on a photon (a) and electron (b) target

Let us look closer at the process depicted in Fig 1. The space-like virtualities of both interacting photons in Fig. 1a are given by

$$Q^2 \equiv -q^2 = -(l-l')^2\,, \tag{1}$$
$$-p^2 = -(k-k')^2 \leq P^2 \tag{2}$$

according to the notation in the figure. P^2 denotes the maximal virtuality of the "target" photon and its value is usually set by experiment (*e.g.* by "anti-tagging" condition).

The measured cross-section for this deep inelastic positron-electron scattering corresponds to Fig. 1b and reads

$$\frac{d\sigma}{dQ^2dz} = \frac{2\pi\alpha^2}{z\,Q^4}\left[(1+(1-y)^2)F_2^e(z,Q^2,P^2) - y^2F_{\rm L}^e(z,Q^2,P^2)\right], \tag{3}$$

where

$$z = \frac{Q^2}{2\,kq} \tag{4}$$

is the fractional parton momentum with respect to the target electron and

$$y = \frac{kq}{kl}. \tag{5}$$

Experimentally y is very small and

$$\frac{d\sigma}{dQ^2dz} \approx \frac{4\pi\alpha^2}{z\,Q^4}\,F_2^e(z,Q^2,P^2). \tag{6}$$

Thus in practice we measure the electron structure function F_2^e, which equals to

$$F_2^e(z,Q^2,P^2) = z\sum_q e_q^2 f_q^e(z,Q^2,P^2). \tag{7}$$

The sum in Eq. (7) runs over all quarks and anti-quarks and $f_q^e(z,Q^2,P^2)$ denotes their distribution inside the electron. This function depends on P^2, because the cross-section is integrated over the target photon virtualities. Thus if we assume that only real photons contribute we need $P^2 \ll Q^2$. How well this is fulfilled experimentally is another question.

The standard approach aims at extracting the photon structure function from the experimental data. To this end one uses the Weizsäcker–Williams approximation [3]

$$f_q^{e^-}\left(z,Q^2,P^2\right) = \int\limits_z^1 \frac{dx}{x} f_q^\gamma\left(x,Q^2\right)\, f_\gamma^{e^-}\left(\frac{z}{x},P^2\right), \tag{8}$$

where $f_\gamma^{e^-}$ is the spectrum of equivalent photons and f_q^γ is the density of quarks inside the photon.

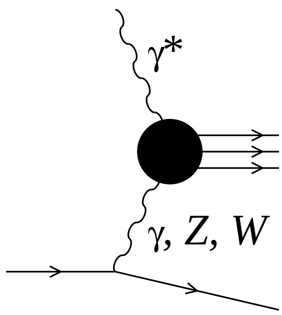

Fig. 2. γ, Z, W contributions to the $\gamma^* e^-$ scattering

At very high energies, however, also Z^0 and W^- bosons can be emitted by the electron (see Fig. 2). On top of that Z^0 and γ have to interfere according to the Standard Model. The Eq. (8) becomes now [4]

$$f_q^{e^-}(z,Q^2,P^2) = \sum_{\substack{A,B= \\ \gamma,Z^0,W^-}} \int\limits_z^1 \frac{dx}{x} f_q^{AB}(x,Q^2)\, F_{AB}^{e^-}(z/x,P^2), \tag{9}$$

where $F_{AB}^{e^-}$ is the density matrix of equivalent bosons and f_q^{AB} describes the number of quarks in this "cloud". Although both of these functions are well defined within QED and QCD the probabilistic (partonic) picture is lost. It gets recovered in the language of the electron structure function. What is important, the γ-Z interference is large and it cannot be neglected.

The QCD content of electron can be calculated in perturbative QCD with the same accuracy as for the photon. The first step is to derive the splitting

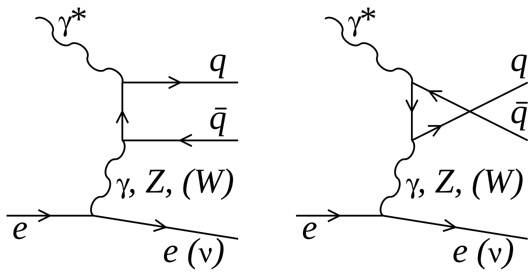

Fig. 3. Feynman diagrams contributing to the electron → quark/anti-quark splitting functions

functions of the electron into quark and anti-quark. For fully polarized case we denote them by $\mathcal{P}_{q_\eta}^{e^-_\lambda}(P^2)$, where η and λ are quark and electron helicities, respectively. The corresponding Feynman diagrams are shown in Fig. 3 and for unpolarized electron the result reads [4]

$$\begin{aligned}
\mathcal{P}_{q_+}^{\mathrm{e}^-}(z,P^2) &= \frac{3\alpha}{4\pi}\Big\{ e_q^2\left[\Phi_+(z)+\Phi_-(z)\right]\log\mu_0 \\
+e_q^2 &\quad \tan^4\theta_{\mathrm{W}}\left[\Phi_+(z)+\rho_{\mathrm{W}}^2\Phi_-(z)\right]\log\mu_{\mathrm{Z}} \\
-2e_q^2 &\quad \tan^2\theta_{\mathrm{W}}\left[-\Phi_+(z)+\rho_{\mathrm{W}}\Phi_-(z)\right]\log\mu_{\mathrm{Z}}\Big\}\,,
\end{aligned} \tag{10a}$$

$$\begin{aligned}
\mathcal{P}_{q_-}^{\mathrm{e}^-}(z,P^2) &= \frac{3\alpha}{4\pi}\Big\{ e_q^2\left[\Phi_+(z)+\Phi_-(z)\right]\log\mu_0 \\
+z_q^2 &\quad \tan^4\theta_{\mathrm{W}}\left[\Phi_-(z)+\rho_{\mathrm{W}}^2\Phi_+(z)\right]\log\mu_{\mathrm{Z}} \\
+2e_qz_q &\quad \tan^2\theta_{\mathrm{W}}\left[-\Phi_-(z)+\rho_{\mathrm{W}}\Phi_+(z)\right]\log\mu_{\mathrm{Z}} \\
+ &\quad (1+\rho_{\mathrm{W}})^2\Phi_+(z)\delta_{q\mathrm{d}}\log\mu_{\mathrm{W}}\Big\}\,,
\end{aligned} \tag{10b}$$

where

$$\begin{aligned}
\Phi_+(z) &= \frac{1-z}{3z}(2+11z+2z^2)+2(1+z)\log z\,, \\
\Phi_-(z) &= \frac{2(1-z)^3}{3z}\,,
\end{aligned}$$

and

$$\mu_0 = \frac{P^2}{m_e^2 z^2/(1-z)}\,, \qquad \mu_{Z/W} = \frac{P^2 + M_{Z/W}^2}{M_{Z/W}^2}\,. \tag{11}$$

$$z_q = \frac{T_3^q}{\sin^2\theta_{\rm W}} - e_q\,, \qquad \rho_{\rm W} = \frac{1}{2\sin^2\theta_{\rm W}} - 1 \tag{12}$$

with $e_q =$ quark charge$/e$, $T_3^q =$ 3-rd weak isospin component and $\theta_{\rm W}$ — the Weinberg angle. These splitting functions depend on P^2 and for very large P^2 the contributions from the weak bosons become comparable to that of photon.

The next step consists in solving the evolution equations for polarized electron structure function [4]:

$$\frac{df_{q_\eta}^{e_\lambda^-}(t)}{dt} = \frac{\alpha}{2\pi}\mathcal{P}_{q_\eta}^{e_\lambda^-}(P^2) + \frac{\alpha_{\rm s}(t)}{2\pi}\sum_{k,\rho} P_{q_\eta}^{k_\rho} \otimes f_{k_\rho}^{e_\lambda^-}(t)\,, \tag{13}$$

$$\frac{df_{G_\eta}^{e_\lambda^-}(t)}{dt} = \frac{\alpha_{\rm s}(t)}{2\pi}\sum_{k,\rho} P_{G_\eta}^{k_\rho} \otimes f_{k_\rho}^{e_\lambda^-}(t), \tag{14}$$

where $t = \log(Q^2/\Lambda_{\rm QCD}^2)$, $\alpha_{\rm s}(t)$ is the QCD running coupling constant and $P_{i_\eta}^{k_\rho}$ denote the polarized QCD splitting functions (Altarelli–Parisi probabilities).

For $\Lambda_{\rm QCD}^2 \ll P^2 \ll Q^2$ the "asymptotic" solutions can be found in the form

$$f_k^{e^-}(z, Q^2, P^2) \simeq \frac{1}{2}\left(\frac{\alpha}{2\pi}\right)^2 f_k^{\rm as}(z)\,\log\frac{Q^2}{\Lambda_{\rm QCD}^2}\log\frac{P^2}{\Lambda_{\rm QCD}^2}\,, \tag{15}$$

where $f_k^{\rm as}(z)$ can be found numerically [4].

In Fig. 4 we show the quark content of polarized electron. At finite energies the contributions from weak bosons are suppressed by the logarithmic factors present in Eq. (10). Nevertheless the γ-Z interference term remains of the same order of magnitude as the Z-Z one. The pure $\gamma\gamma$ contribution cancels out in the left-right asymmetry, $(e_{\rm R}^- - e_{\rm L}^-)/2$. It would be interesting to measure it in next generation experiments.

At presently available energies only photons contribute to the electron structure function and thus for small P^2 it can be expressed in terms of the photon structure function $f_k^\gamma\left(x, Q^2\right)$, where x is the fractional parton momentum with respect to the photon. To extract it from the experimental data we use the formula (for $P^2 \ll Q^2$)

$$x = \frac{Q^2}{M_X^2 + Q^2}\,, \tag{16}$$

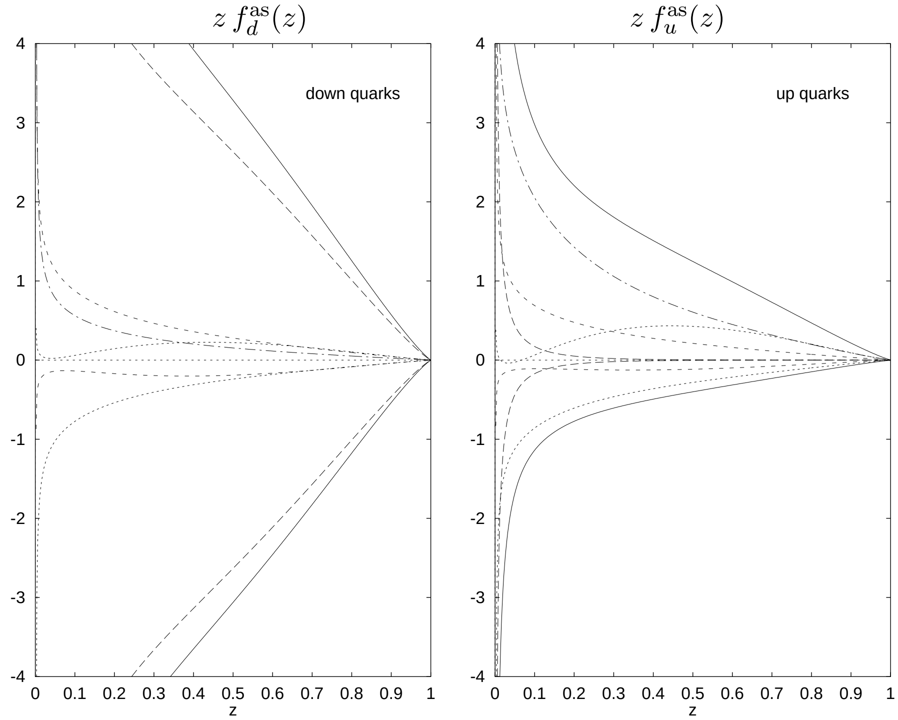

Fig. 4. Asymptotic electron structure function. The positively valued curves show the quark content of unpolarized electron, $(e^-_{\rm R} + e^-_{\rm L})/2$. The negative ones — the left-right asymmetry, $(e^-_{\rm R} - e^-_{\rm L})/2$. Full lines give the asymptotic result with all γ, Z and W included. The other curves give the contributions from: $\gamma\gamma$ — dashed-dotted; γZ — dotted; ZZ — short dashed; WW — long dashed.

where M_X is the invariant mass of final hadronic state X shown in Fig. 1a. This mass is difficult to measure which results in big errors on x. On the contrary, there is no need to measure x to obtain the electron structure function. It seems thus that the same experiment should provide more precise data for the electron structure than for the photon one.

Let us add a final remark on the virtual photon structure function [5]. In terms of the electron structure function the effects of the photon virtuality are taken into account by the dependence on P^2. This time, however, we study a real, convention independent object. Even when there is no Z admixture, the whole range of target photon virtualities is properly taken into account.

REFERENCES

[1] E. Witten, *Nucl. Phys.* **B120**, 189 (1977); C.H. Llewellyn-Smith, *Phys. Lett.* **79B**, 83 (1978); R.J. DeWitt *et al.*, *Phys. Rev.* **D19**, 2046 (1979); T.F. Walsh, P. Zerwas, *Phys. Lett.* **36B**, 195 (1973); R.L. Kingsley, *Nucl. Phys.* **B60**, 45 (1973).

[2] H.J. Behrend *et al.*, CELLO Collaboration, *Phys. Lett.* **126B**, 391 (1983); Ch. Berger *et al.*, PLUTO Collaboration, *Phys. Lett.* **142B**, 111 (1984); Nucl. Phys. **B281**, 365 (1987); W. Bartel *et al.*, JADE Collaboration, *Z. Phys.* **C24**, 231 (1984); M. Althoff *et al.*, TASSO Collaboration, *Z. Phys.* **C31**, 527 (1986); H. Aihara *et al.*, TPC/2γ Collaboration, *Z. Phys.* **C34**, 1 (1987); *Phys. Rev. Lett.* **58**, 97 (1987); T. Sasaki *et al.*, AMY Collaboration, *Phys. Lett.* **252B**, 491 (1990); R. Akers *et al.*, OPAL Collaboration, *Z. Phys.* **C61**, 199 (1994); S.K. Sahu *et al.*, AMY Collaboration, *Phys. Lett.* **B346**, 208 (1995); P. Abreu *et al.*, DELPHI Collaboration, *Z. Phys.* **C69**,223 (1996); K. Ackerstaff *et al.*, OPAL Collaboration, *Z. Phys.* **C74**, 33 (1997); *Phys. Lett.* **B411**, 387 (1997); *Phys. Lett.* **B412**, 225 (1997).

[3] C.F. von Weizsäcker *Z. Phys.* **88**, 612 (1934); E.J. Williams, *Phys. Rev.* **45**, 729 (1934).

[4] W. Słomiński, J. Szwed, *Phys. Lett.* **B387**, 861 (1996); *Acta Phys. Pol.* **B27**, 1887 (1996).

[5] T. Uematsu, T.F. Walsh, *Phys. Lett.* **B101**, 263 (1981); F.M. Borzumati, G.A. Schuler, *Z. Phys.* **C58**, 139 (1993). M. Drees, R.M. Godbole, *Phys. Rev.* **D50**, 3124 (1994).